Theor Chim Acta (1986) 69: 409–423

Theoretica Chimica Acta

Dimer coverings and Kekulé structures on honeycomb lattice strips*

D. J. Klein, G. E. Hite, W. A. Seitz and T. G. Schmalz

Theoretical Chemical-Physics Group, Department of Marine Sciences, Texas A and M University at Galveston, Galveston, TX 77553, USA

(Received August 26, 1985/Accepted January 6, 1986)

The problem of covering every site of a subsection of the honeycomb lattice with disjoint edges is considered. It is pointed out that a type of long-range order associated to such coverings can occur, so that different phases can arise as a consequence of the subsection's boundaries. These features are quantitatively investigated via a new analytic solution for a class of strips of arbitrary widths, arbitrary lengths, and arbitrary long-range-order values. Relations to work on the dimer covering problem of statistical mechanics and especially to the resonance theory of benzenoid hydrocarbons are noted.

Key words: Kekulé structure enumeration — Dimer covering enumeration — 1-Factor enumeration — Benzenoid π-network polymers — Long-range order — Bond localization — Edge reactivity — Graph theory — Transfer matrices

1. Introduction

A general problem of interest in chemistry, physics, and mathematics is to enumerate the number of ways of choosing bonds from a network such that each node of the network has a single chosen bond incident upon it. In organic chemistry such choices for bonds of a π-network (of sp^2-hydridized carbon atoms) are termed *Kekulé structures.* In statistical mechanics such structures are termed *dimer coverings* (representing a monolayer of diatoms on a lattice surface). In mathematics these structures are termed *perfect matchings* or *1-factorizations* of a graph. The logarithm of the number of these structures is (proportional to) the conformational entropy in statistical mechanics, and in organic chemistry it is related to the system's "resonance energy".

* Supported by The Robert A. Welch Foundation of Houston, Texas

A variety of different enumeration methods have been developed for these Kekulé structures or dimer coverings:

(a) several graph-theoretic combinatorial recursion methods [1–10] typically for rather special subclasses of graphs relevant in organic chemistry, or narrow strips of interest in statistical mechanics [11–14];

(b) a special technique [2, 5, 15–17] involving correspondences to a collection of self-avoiding walkers, evidently limited to certain subsections of the honeycomb (or graphite) lattice;

(c) a determinantal method [2, 6, 18–20] where the square of the desired count is obtained as the determinant of the graph's adjacency matrix, being primarily restricted to the "benzenoid" graphs of organic chemistry;

(d) a Pfaffian [21, 22] and a related permanental [23] method best applicable to bipartite planar graphs, especially with translational symmetry (and "cyclic" boundary conditions);

(e) a transfer matrix method [24], such as is often applied to other translationally symmetric statistical mechanical problems;

(f) a method [25–30] based upon the enumeration of the much less numerous "Clar" graphs, though apparently simply applicable only to special subclasses of benzenoid structures;

(g) several other methods [31–35] based upon solutions of other (equivalent or related) transformed problems, especially in the case of subsections of the honeycomb lattice;

(h) some additional methods [20, 36–39] based upon computer intensive counting, but applicable to rather arbitrary not overly large benzenoid subgraphs.

Often these various methods of solution seem to have been developed (occasionally with some duplication) independently in either organic chemistry or statistical mechanics.

In both fields it has been noted that there are some unusual features which arise with subsections of the honeycomb (or graphite) lattice. This problem concerns the effect of the boundary upon the enumeration. Thus, Stein and Brown [20] note that the enumeration appears to extrapolate to different large lattice limits, depending upon the shape of the edges. They suggest that "even in arbitrarily large graphite layers, average π-electron energies may depend upon the nature of the edges". Correspondingly Elser [34, 40] obtains a boundary-dependent enumeration and says that "a bulk limit of the entropy does not exist". Later choosing the boundary to maximize his entropy per site Elser obtains a value substantially less than that previously found [34] for a lattice with cyclic boundary conditions.

In fact these seemingly anomalous results for the honeycomb lattice are linked to a type of long-range order, which has already been discussed [41–44] for the occurrence of "solitonic" excitations in π-network polymers. This *long-range*

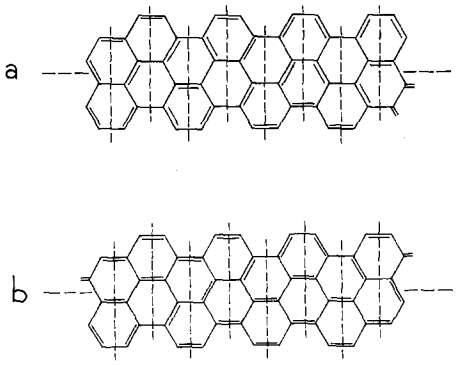

Fig. 1. Two representative Kekulé structures on a width $w=3$ strip. The structures have $Q=1$ and $Q=2$ bonds (in a and b) at each position along the strip

order is most easily introduced in terms of examples on narrow strips cut from the honeycomb lattice. Thus, in Fig. 1a the type of Kekulé structure (or dimer covering) shown there has one longitudinal π-bond (or dimer) at each position along the strip as marked by a transverse dotted line. But the type of structure in Fig. 1b has two longitudinal π-bonds at each position. The crucial point here is that there are no Kekulé structures that have different numbers of longitudinal π-bonds at different positions. The number of such bonds at any position along the strip will be denoted by Q. For a strip of width w it can be seen that Q may vary from 0 to w depending upon the nature of the strip ends. (Also, this long-range-order feature is closely related to the enumeration procedure of (b) involving [2, 15–17] a correspondence to Q self-avoiding directed walkers; the retention of our long-range-order is equivlaent to the conservation of walkers.)

Here for such subsections of the honeycomb lattice we explicitly enumerate the number of Kekulé structures for arbitrary choices of the long-range-order parameter Q, arbitrary strip widths w, and arbitrary strip lengths L. Allowance is made for a variety of different types of strip ends. As a consequence the different anomalies noted earlier are clarified. It is argued that, at least physically and chemically, there *are* bulk limits for entropy (and resonance energy), and the manner of approach of the solution to that obtained with cyclic boundary conditions is found. As a further point of interest some notable oscillations in bond orders are studied.

The analytic solution behind these observations proceeds via a transfer matrix method, which has not previously been applied to the honeycomb lattice (though it takes a "simple" form related to many-body methodology for Q independent particles).

2. Transfer matrix formulation

The formulation of the problem in an amenable manner proceeds via a consideration of the local nature of a Kekulé structure at a position along the length of the strip. At such a longitudinal position there will be Q longitudinal π-bonds (or dimers) occupying the w longitudinal network bonds available there.

The *local state* at this longitudinal position is then indicated as

$$|m_1, m_2, \ldots, m_Q) \equiv |m(Q)) \tag{2.1}$$

in terms of the ordered transverse positions $m_1, m_2, \ldots, m_Q$ of these π-bonds. With the network bonds positioned sequentially from 1 to w, as in Fig. 2, the local state of (2.1) satisfies

$$0 < m_1 < m_2 < \cdots < m_Q \leq w. \tag{2.2}$$

Because of the effective glide-plane translational symmetry along the strip, the transverse positions at the next longitudinal position are reversed, as indicated in Fig. 2a. For example the $Q = 3$ local states in Fig. 2b are $|4, 5, 8)$ and $|2, 5, 7)$ at the longitudinal positions on the left and right, respectively.

Next we note the correlations between one local state and the one at an adjacent (longitudinal) position. Only certain $|p(Q))$ may follow a given $|m(Q))$. In particular if we define intervals of successive integers

$$I(m_{i-1}, m_i) \equiv \{w - m_i + 1, \ldots, w - m_{i-1}\}, \qquad i = 1 \text{ to } Q \tag{2.3}$$

(with $m_0 \equiv 0$), then it turns out that $|p(Q))$ can follow $|m(Q))$ if [41]

$$p_{Q-i+1} \in I(m_{i-1}, m_i), \qquad i = 1 \text{ to } Q. \tag{2.4}$$

This is most readily understood from a "geometrical" examination of the circumstance in Fig. 2b where for $|m(3)) = |4, 5, 8)$ one sees that the 12 adjacent allowed local states are $|p_1, 5, p_3)$ with

$$p_1 \in \{2, 3, 4\} = I(5, 8) \quad \text{and} \quad p_3 \in \{6, 7, 8, 9\} = I(0, 4). \tag{2.5}$$

The set of conditions of (2.4) may be succinctly summarized by saying that $m(Q)$ and $p(Q)$ *interlace*

$$w \geq p_Q > w - m_1 \geq p_{Q-1} > w - m_2 \geq \cdots \geq p_1 > w - m_Q \geq 0, \tag{2.6}$$

a relation which actually is symmetrical with respect to $m(Q)$ and $p(Q)$.

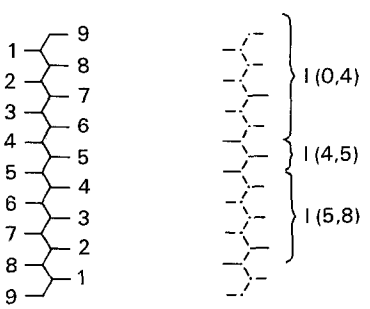

Fig. 2. Structures to identify a local state at a position along a strip (of width $w = 9$), as discussed in the text

The *transfer matrix* acting on the space of local states has elements identifying allowed "adjacencies"

$$(p(Q)|\boldsymbol{T}|m(Q)) = \begin{cases} 1, & p(Q) \text{ interlaces } m(Q), \\ 0, & \text{otherwise.} \end{cases} \tag{2.7}$$

Now applying $\boldsymbol{T}$ to $|m(Q))$ l times gives a vector whose $p(Q)$th component $(p(Q)|\boldsymbol{T}^l|m(Q))$ is the number of ways that a local state $|p(Q))$ can follow $|m(Q))$ at a distance l farther down the strip. As a consequence, the total number of Kekulé structures on a strip with L longitudinal positions is given as

$$N_Q(w, L) = (t|\boldsymbol{T}^{L-1}|i), \tag{2.8}$$

where $|i)$ and $|t)$ are initiating and terminating vectors whose components identify the permissible arrangements for longitudinal π-bonds at the extreme ends of the strip. Generally the forms of $|i)$ and $|t)$ depend upon the particular nature of the strip ends, which also determine the relevant value of Q (at least if a global Kekulé structure is sought).

The eigenvalue problem for $\boldsymbol{T}$

$$\boldsymbol{T}|\lambda) = \lambda|\lambda) \tag{2.9}$$

can be used to recast the enumeration expression in a convenient form. Indeed if the eigenvectors are orthonormalized (as they surely can be since the symmetry of the interlacing relation implies $\boldsymbol{T}$ is Hermitian), then

$$N_Q(w, L) = \sum_{\lambda} (t|\lambda)(\lambda|i)\lambda^{L-1}. \tag{2.10}$$

Further, for sufficiently long strips the maximum (magnitude) eigenvalue Λ_Q dominates, so that

$$N_Q(w, L) \to (t|\Lambda_Q)(\Lambda_Q|i)\Lambda_Q^{L-1}, \qquad \text{as } L \to \infty \tag{2.11}$$

is accurate to within a vanishingly small percentage error.

3. Analytic solution

The solution to the eigenvalue problem for general Q is developed by embedding the present problem in another on a larger vector space. This larger "Q-particle" space has a basis of direct products

$$|m_1 \times m_2 \times \cdots \times m_Q\rangle \equiv |m_1\rangle \times |m_2\rangle \times \cdots \times |m_Q\rangle \tag{3.1}$$

of (orthonormal) "1-particle" basis vectors

$$|m_i\rangle, \qquad m_i = 1 \text{ to } w, \quad i = 1 \text{ to } Q. \tag{3.2}$$

The product space contains an antisymmetric subspace, with basis vectors

$$|m(Q)\rangle \equiv \frac{1}{\sqrt{Q!}} \sum_{\pi} (-1)^{\pi} \pi |m_1 \times m_2 \times \cdots \times m_Q\rangle,$$

$$0 < m_1 < m_2 < \cdots < m_Q \leq w, \tag{3.3}$$

where the sum is over Q-particle permutations π acting on the "particle positions". This antisymmetric subspace corresponds in a natural way to the local-state space of section 2,

$$|m(Q)\rangle \leftrightarrow |m(Q)) \tag{3.4}$$

since the m_i are subject to the same constraints in both spaces.

Next we consider a Q-fold direct product matrix

$$(\tau)^{\times Q} \equiv \tau \times \tau \times \tau \times \cdots \times \tau \tag{3.5}$$

acting on the (Q-particle) direct-product space. Here the 1-particle operator τ is the same as a $Q=1$ transfer matrix

$$\langle p|\tau|m\rangle = \begin{cases} 1, & w \geq p > w-m \geq 0, \\ 0, & \text{otherwise.} \end{cases} \tag{3.6}$$

Clearly $(\tau)^{\times Q}$ commutes with the permutations π and so leaves the antisymmetric subspace of (3.3) invariant. To establish the representation of $(\tau)^{\times Q}$ on this antisymmetric subspace we examine the matrix elements

$$\begin{aligned} \langle p(Q)|(\tau)^{\times Q}|m(Q)\rangle &= \frac{1}{Q!}\sum_{\pi,\pi'}(-1)^{\pi\pi'}\langle p_1 \times \cdots \times p_Q|\pi^{\dagger}(\tau)^{\times Q}\pi'|m_1 \times \cdots \times m_Q\rangle \\ &= \sum_{\pi}(-1)^{\pi}\langle p_1 \times \cdots \times p_Q|\pi(\tau)^{\times Q}|m_1 \times \cdots \times m_Q\rangle \\ &= \sum_{n_1}^{>w-m_1} \cdots \sum_{n_Q}^{>w-m_Q} \sum_{\pi}(-1)^{\pi}\langle p_1 \times \cdots \times p_Q|\pi|n_1 \times \cdots \times n_Q\rangle \end{aligned} \tag{3.7}$$

where the m_i are an increasing sequence so that the ranges of summation for the n_i decrease with increasing i. There are some index sets $n_1, \ldots, n_Q$ that occur only once in the Q-fold n_i-sums of (3.7); these index sets are those with $n_i \in I(m_{i-1}, m_i)$, $i=1$ to Q. Other index sets arising in the Q-fold sums, i.e., those with two or more n_j in some of the $I(m_{i-1}, m_i)$, arise repeatedly with their arguments permuted about such that half the permutations are odd and half are even. (Such a division into different parity permutations follows since the set of these permutations form a group which is just a product of "symmetric" groups, which so divide.) Now when two or more n_j occur in some of the $I(m_{i-1}, m_i)$ and when the index set coincides with that of $p(Q)$, for every permutation π carrying one of the sequences to $p(Q)$ there will be an opposite parity permutation (differing from π by an initial transposition of two n_j in the same interval $I(m_{i-1}, m_i)$) carrying another sequence to $p(Q)$; and hence the matrix element will be zero. The nonzero matrix elements will have a sign $(-1)^{\sigma}$ where σ is the permutation that reorders $n(Q)$ to $n'(Q) \equiv n_Q, n_{Q-1}, \ldots, n_1$. This permutation σ evidently consists of disjoint transpositions whose number is i$(Q/2)$, the integer part of $Q/2$. Thus we have

$$\langle p(Q)|(\tau)^{\times Q}|m(Q)\rangle = \begin{cases} (-1)^{\mathrm{i}(Q/2)}, & m(Q) \text{ interlaces } p(Q) \\ 0, & \text{otherwise.} \end{cases} \tag{3.8}$$

Using $[\cdot]^A$ to indicate a restriction to the antisymmetric subspace and comparing (3.8) with (2.7), we find

$$[(\boldsymbol{\tau})^{\times Q}]^A = (-1)^{\mathrm{i}(Q/2)}\boldsymbol{T} \tag{3.9}$$

a simple relation to the desired transfer matrix.

Because the antisymmetric subspace is invariant under $(\boldsymbol{\tau})^{\times Q}$, the eigensolutions of $[(\boldsymbol{\tau})^{\times Q}]^A$ are just a subset of those of $(\boldsymbol{\tau})^{\times Q}$. In particular the eigenvalues are just products of those λ_k, $k=1$ to w, for $\boldsymbol{\tau}$. Then the eigenvalues of $\boldsymbol{T}$ are

$$\lambda_{k(Q)} = (-1)^{\mathrm{i}(Q/2)} \prod_{i=1}^{Q} \lambda_{k_i}, \qquad 0 < k_1 < k_2 < \cdots < k_Q \leq w \tag{3.10}$$

and the corresponding eigenvector's components are

$$(m(Q)|\lambda_{k(Q)}) = \langle m(Q)|\lambda_{k(Q)}\rangle = \det\{\langle m_i|\lambda_{k_j}\rangle\} \tag{3.11}$$

where the "Slater determinant" here is that of the matrix with (i,j)th element $\langle m_i|\lambda_{k_j}\rangle$.

Finally the eigenvalues to $\boldsymbol{\tau}$ are

$$\lambda_k = (-1)^{k+1} \Big/ 2\sin\left(\frac{2k-1}{2w+1}\frac{\pi}{2}\right), \qquad k=1 \text{ to } w \tag{3.12}$$

and the orthonormal eigenvector components are

$$\langle m|\lambda_k\rangle = \frac{2}{\sqrt{2w+1}} \sin\left(\frac{2k-1}{2w+1} m\pi\right), \qquad m=1 \text{ to } w. \tag{3.13}$$

The validity of these equations may be checked upon application of (3.6) to these vectors $|\lambda_k\rangle$ specified by (3.13).

4. Approaching the bulk limit

For very long strips the Kekulé count is dominated by the maximum eigenvalue

$$\Lambda_Q = 2^{-Q}\left\{\prod_{k=1}^{Q} \sin\left(\frac{2k-1}{2w+1}\frac{\pi}{2}\right)\right\}^{-1} \tag{4.7}$$

as results from (3.10) and (3.12). This eigenvalue, and hence the Kekulé count, then increases monotonically with increasing Q for $Q \leq (w-1)/3$, and following this it decreases monotonically with Q. That the maximum in Λ_Q occurs at $w/Q = \frac{1}{3}$ as $w \to \infty$ is simply an indication that on the graphite lattice most Kekulé structures have π-bonds with equal likelihood in each of the three equivalent directions.

Another point of interest [41-44] is the possibility of degeneracy of two maximum-cardinality Kekulé phases. Such a cardinality degeneracy occurs asymptotically when

$$2\sin\left(\frac{2Q+1}{2w+1}\frac{\pi}{2}\right) = \frac{\Lambda_Q}{\Lambda_{Q+1}} = 1 \tag{4.2}$$

as happens for integer w and Q if and only if

$$w = 3n+1, \qquad n = 0, 1, 2, 3, \ldots \tag{4.3}$$

whence the two maximum-cardinality degenerate phases have $Q=n$ and $Q=n+1$. Such degeneracies (or more likely near-degeneracies for more realistic resonance-energy computations) have implications [42–44] for the possibility of solitonic excitations in the corresponding polymeric π-network strips. (See the accompanying paper "Extended π-networks with multiple spin-pairing phases: resonance-theory calculations on poly-polyphenanthrenes" in this journal.)

In the large network limit ($L\to\infty$ and $w\to\infty$) the Kekulé count further asymptotically factors with regard to a power of w. The resulting size consistent asymptotic expression is

$$\{N_Q(w,L)\}^{1/wL}\to\Lambda_Q^{1/w}\to\exp-\left\{\frac{Q}{w}\ln 2+\frac{2}{\pi}\int_0^{\pi Q/2w}\ln(\sin x)\,dx\right\}, \tag{4.4}$$

which is plotted in Fig. 3. The maximum value (at $Q/w=\frac{1}{3}$) of ~1.3813564 yields the previous [15, 22, 32] counts for a honeycomb lattice with cyclic boundary conditions. (Note that the logarithm of the expression in (4.4) is the entropy per dimer.) This then illustrates that the entropy per site on a section of the honeycomb lattice is not limited to the (smaller) maximum value found by Elser [34].

It is to be emphasized that in the infinite lattice limit the entropy per site, or resonance energy, is quite well-defined, at least in a chemical or physical sense. Basically the energy cost of unpaired sites near the boundary is negligible in this limit, so long as the number of such sites scales no faster than the boundary length, which itself approaches an infinitesimal fraction of the whole. (This also requires that the absolute temperature be positive for the statistical mechanical application, and for the organic chemical application that the excitation energy for unpaired π-electrons be finite.) Then such unpaired sites may be introduced so as to achieve the maximum cardinality Q-phase with a vanishingly small cost to the (free or resonance) energy per site. Hence the bulk limit is obtained the same as for a system with cyclic boundary conditions. With open ends the (relatively few) unpaired sites near the boundary may be expected to exhibit unusual reactivity.

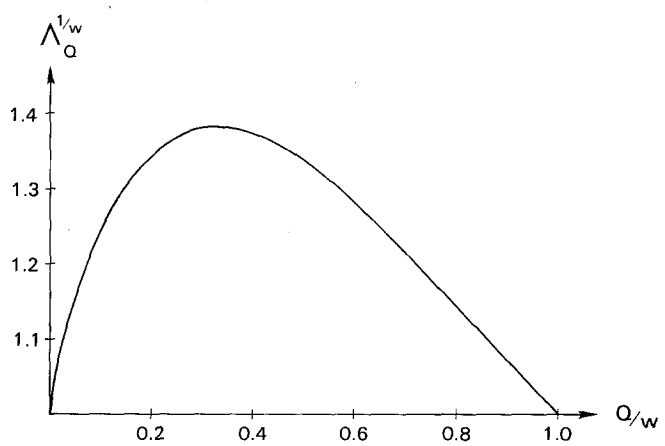

Fig. 3. Asymptotic number of Kekulé structures per bond, for the extended honeycomb (or graphite) lattice

A further point is that partition functions with different weights (or activities) x and y for longitudinal and diagonal dimers may be constructed. For the chain with cyclic boundary conditions at the strip ends this is

$$Z_{w,L}(x, y) = \sum_{Q=0}^{w} x^{QL} y^{(2w-2Q)L} N_Q(w, L) \tag{4.5}$$

the result for w, $L \to \infty$ then corresponding to previous work [15, 21, 22, 31, 32].

5. Strip ends and finite strips

For smaller networks, or any circumstance where a global Kekulé structure is sought, the boundaries determine Q. For our strips the determining feature is the nature of the strip ends (at the extreme left and right in Figs. 1 and 2). For the strip ends of Fig. 4a–d the associated respective Q-values are $Q = 1$, $Q \cong w/3$, $Q \cong w/2$, and $Q \cong w/3$. Thus edges as in b or d lead to greater counts than those in a or c, as is consistent with Brown and Stein's extrapolations [20] involving edges of types a, b and c. Another preferred type of edge is that occurring on the longitudinal sides of our strips.

For the type of strips considered here if the ends admit a particular value for the long-range order parameter Q, then the Kekulé structure enumeration is given exactly as

$$N_Q(w, L) = \sum_{k(Q)} (t|\lambda_{k(Q)})(\lambda_{k(Q)}|i) 2^{-Q(L-1)} \prod_{i=1}^{Q} \left\{ \sin \frac{2k_i - 1}{2w+1} \frac{\pi}{2} \right\}^{-L+1}, \tag{5.1}$$

where the sum is over all ordered sequences $k(Q)$ of distinct integers $0 < k_1 < k_2 < \cdots < k_Q \leq w$. All the information concerning the strip ends is bound up in the value of Q and the coefficients $(t|\lambda_{k(Q)})(\lambda_{k(Q)}|i)$ which are independent of the strip length L and which are a maximum for the dominant eigenvalue. This latter

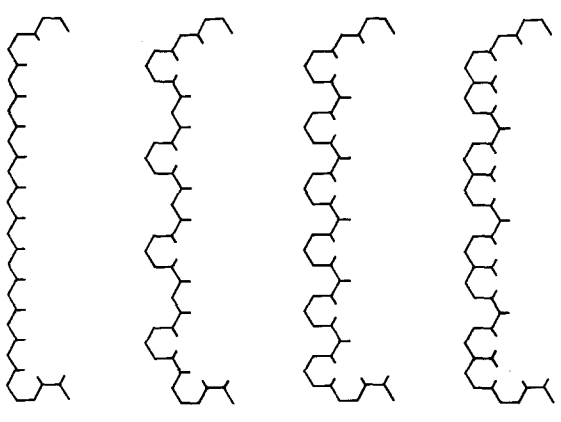

Fig. 4. A variety of strip ends

point is seen because the components of the corresponding eigenvector are all positive (as established by the Frobenius-Perron theorem [45]), and because the components of $|i)$ and $|t)$ are all non-negative. (The remaining non-maximum-eigenvalue eigenvectors being orthogonal to $|\Lambda_Q)$ have comparable quantities of components of both signs, and so *tend* toward orthogonality to $|i)$ and $|t)$ too.)

As an example for the $Q=1$ edge of Fig. 4a the single longitudinal bond may be in any transverse position, so that $|t)=|i)=\boldsymbol{T}|w)$, and we have

$$(t|\lambda_k)(\lambda_k|i)=\lambda_k^2(w|\lambda_k)(\lambda_k|w)=\frac{1}{2w+1}\cot^2\left(\frac{2k-1}{2w+1}\frac{\pi}{2}\right), \tag{5.2}$$

which may be seen to be quite sharply peaked at the maximum ($k=1$) eigenvalue. Then the explicit enumeration for this class is

$$N_1(w,L)=\frac{1}{2w+1}\sum_{k=1}^{w}\cot^2\left(\frac{2k-1}{2w+1}\frac{\pi}{2}\right)\left\{2\sin\left(\frac{2k-1}{2w+1}\frac{\pi}{2}\right)\right\}^{-L+1} \tag{5.3}$$

the $w=1$, 2, and 3 subclasses have been previously treated [2, 5, 9] somewhat differently by methods which do not so explicitly manifest the asymptotic $L\to\infty$ behavior, though they typically display more explicitly the count as an integer. A further comment in connection with (5.3) is that (at least for long strips) $\Lambda^{1/w}$ approaches unity as $w\to\infty$ so that [42] this class is not a *size-consistent* basis for computing energies, in the sense that the difference between the resultant energy per site and that of a single Kekulé structure approaches 0 (as $L\to\infty$). Again in such circumstances unpaired (at least to nearest neighbors) sites near the ends of the strip should appear giving rise to an overall lower energy (per site).

Development of expressions for yet other types of ends simply involves further choices of the end states $|i)$ and $|t)$ followed by evaluation of the coefficients $(t|\lambda_{k(Q)})(\lambda_{k(Q)}|i)$. To do this it is frequently possible and convenient to introduce more "primitive" end states $|i-)$ and $|t-)$ corresponding to specifications one step farther back, i.e., to the left of the "lettered" state positions in Fig. 4. Then

$$\begin{aligned}
&|i)=\boldsymbol{T}|i-)\\
&|t)=\boldsymbol{T}|t-)\\
&(t|\lambda_{k(Q)})(t|\lambda_{k(Q)})=\lambda_{k(Q)}^2(t-|\lambda_{k(Q)})(\lambda_{k(Q)}|i-).
\end{aligned} \tag{5.4}$$

For the case of Fig. 4b

$$|i-)=\sum_{p_1=2}^{3}\sum_{p_2=5}^{6}\cdots\sum_{p_Q=3Q-1}^{3Q}|p(Q)), \tag{5.5}$$

where $Q=i[w/3]$. Then, using standard methods for dealing with Slater determinants, one finds

$$(\lambda_{k(Q)}|i-)=\left(\frac{2}{\sqrt{2w+1}}\right)^Q\det\left\{\sin\left[\frac{2k_n-1}{2w+1}(3m-2)\pi\right]+\sin\left[\frac{2k_n-1}{2w+1}(3m-1)\pi\right]\right\}, \tag{5.6}$$

where the term in brackets is the (m, n)th element of the matrix whose determinant

Table 1

	$N_1(4, L)$	$N_2(4, L)$	$[N_1(4, L)]^{1/4L}$	$[N_2(4, L)]^{1/4L}$
1	4	4	1.41421	1.41421
2	10	11	1.33352	1.34950
3	30	31	1.32768	1.33131
4	85	89	1.32004	1.32384
5	246	256	1.31688	1.31951
6	707	737	1.31439	1.31667
7	2 037	2 122	1.31274	1.31466
8	5 864	6 110	1.31146	1.31315
9	16 886	17 593	1.31048	1.31198
10	48 620	50 657	1.30970	1.31104
11	139 997	145 861	1.30905	1.31027
12	403 104	419 990	1.30852	1.30964
13	1 160 693	1 209 313	1.30806	1.30910
14	3 342 081	3 482 078	1.30768	1.30864
15	9 623 140	1 002 6244	1.30734	1.30823
⋮			⋮	⋮
∞			1.30264	1.30264

is being taken. For the circumstance of Fig. 4c a formula similar to (5.6) arises but with the arguments $(3m-2)$ and $(3m-1)$ replaced by $(2m-1)$ and $(2m)$. For the strip end of Fig. 4d a third sine function would appear in each matrix element of the determinant in (5.6). Also for Fig. 4c and d it is convenient to take even a second step back to give even more primitive (yet simpler) initiating states. Of course, if $|i)$ and $|t)$ associate to different Q values, then there are no (global) Kekulé structures. Thus for the various possible distinct pairs of ends from Fig. 4 the only (generally) consistent pair is {4b, d}.

The asymptotic degeneracy of the maximum cardinality Kekulé phases for width $w=3n+1$ infinite strips has a corresponding near degeneracy even for different finite length strips whose end configurations are chosen so as to fix $Q=n$ and $n+1$. Thus, for $Q=1$ (ends of the type in 4a) and $Q=2$ (ends as in Fig. 5), $w=4$ finite strip exact Kekulé counts for strips of up to 15 in length are given in Table 1 along with $[N_Q(4, L)]^{1/wL}$ for comparison with Eq. (4.4).

6. Short-range order

In resonance-theoretic calculations with the valence-bond Hamiltonian for strips of width $w \leq 7$, we have noted that bond orders fluctuate in a rather pronounced

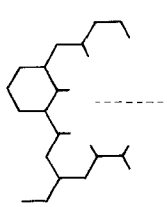

Fig. 5. The $Q=2$ type of strip end used in the computations for Table 1

manner as a function of transverse position across the strip. This feature has an analog in the present Kekulé structure enumeration problem which we can use to elucidate these earlier observations and to extend consideration to wider strips. That is, we here consider the fraction of Kekulé structures which have a π-bond located on a particular longitudinal network bond. This so-called *Pauling bond-order* (for the given lattice bond) is in close quantitative [46–49] correspondence with bond lengths in aromatic benzenoids.

In terms of the transfer matrix formulation of Sect. 2 the number of structures having a π-bond at longitudinal position l and transverse position p is

$$\sum_{m(Q)}^{p} (t|\boldsymbol{T}^{l-1}|m(Q))(m(Q)|\boldsymbol{T}^{L-l}|i), \tag{6.7}$$

where the sum is over all $m(Q)$ that have one of the $m_i = p$. With the supposition that the longitudinal position is well away from both ends, the asymptotic ($L \to \infty$) form of this becomes

$$\sum_{m(Q)}^{p} \Lambda_Q^{l-1}(t|\Lambda_Q)(\Lambda_Q|m(Q))(m(Q)|\Lambda_Q)(\Lambda_Q|i)\Lambda_Q^{L-l}. \tag{6.2}$$

Then taking the ratio of this with $N_Q(w, L)$ as in (2.11), we find the corresponding Pauling bond order (at transverse position p) to be

$$\beta_p = \sum_{m(Q)}^{p} (\Lambda_Q|m(Q))(m(Q)|\Lambda_Q). \tag{6.3}$$

After some manipulation of the determinantal eigenvector solutions of (3.11), or alternatively realizing that (6.3) can simply be viewed as an expectation value of a one-particle number operator for a particle in position p, one obtains

$$\beta_p = \sum_{k=1}^{Q} (\lambda_k|p)(p|\lambda_k). \tag{6.4}$$

Then upon the use of (3.13) and some standard trigonometric manipulations, we find

$$\beta_p = \frac{2Q}{2w+1}\left\{1 - \sin\left(\frac{4Qp}{2w+1}\pi\right)\Big/ 2Q \sin\left(\frac{2p}{2w+1}\pi\right)\right\} \tag{6.5}$$

the desired result for arbitrary Q and w.

The behavior of the bond-order can be further clarified in terms of its fractional fluctuation

$$f_p = \frac{\beta_p - Q/w}{Q/w} \tag{6.6}$$

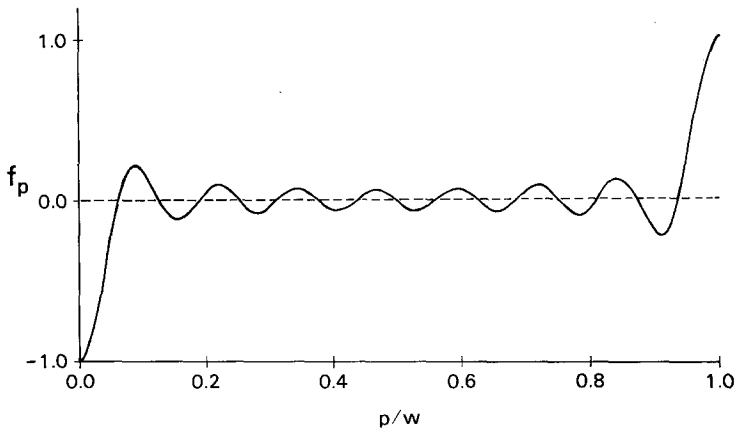

Fig. 6. Bond-order oscillations for strips with $Q=8$

away from its mean value $\bar{\beta}_p = Q/w$. In the limit of very wide strips ($w \to \infty$)

$$f_p \to -\left(\frac{1}{2Q \sin x\pi}\right)(\sin 2Qx\pi), \tag{6.7}$$

where $x \equiv p/w$ is the fractional distance across the strip of position p. Here in (6.7) the first term in parentheses is a slowly varying *envelope* function and the second term in parentheses is a rapidly oscillating function (at least for larger Q, say $Q/w > 0$ as $w \to \infty$) exhibiting the bond-order fluctuations we earlier noted in valence-bond calculations. Here the envelope quenches the oscillations upon moving away from a lateral edge, illustrated for $Q=8$ in Fig. 6. For very wide strips and small x the envelope function reduces to $\cong l/x$ where

$$l = \tfrac{1}{2}\pi Q \tag{6.8}$$

is a *correlation length* (in units of the strip width) for quenching the bond-order oscillations. Initially the oscillation amplitudes die out (with distance from an edge) quite rapidly on a scale of their wavelength, since this wavelength is also l. Over longer lengths this amplitude dies out rather slowly because the functional form l/x for the envelope dies off rather slowly, say when compared with an otherwise common circumstance with a half-length l' and consequent envelope function $2^{-x/l'}$. In narrow strips (or more generally for small Q) the bond-order oscillations are quite notable all the way across the strip. Thence in resonance theory a special pattern of bond length variations is predicted near edges of our present longitudinal type. Likewise in statistical mechanics a type of mean dimer occupancy pattern is predicted.

7. Conclusion

We have established a new analytic enumeration of Kekulé structures (or dimer coverings) on a range of subsections of the honeycomb lattice. The subsections

are of arbitrary width, length, and long-range order, though the width does not vary within one subsection and the lateral edges are of a particular ("corrugated") type. The role of the strip ends is noted to be rather different in the bulk and finite limits, where the restriction to "global" Kekulé structures is, respectively, inappropriate or appropriate. When inappropriate there generally occur a few unpaired sites (with fractional number vanishingly small in the bulk limit) near the strip ends and which as a consequence can be "reactive". With the restriction to global Kekulé structures every single site is paired and the strip ends govern the long-range ordering and a length-independent multiplicative factor in the enumeration formula. The findings clarify several apparent anomalies previously found for the enumeration problem on subsections of the honeycomb lattice.

References

1. Wheland GW (1935) J Chem Phys 3:356
2. Gordon M, Davison WHT (1952) J Chem Phys 20:428
3. Dewar MJS, Longuet-Higgins HC (1952) Proc Roy Soc (London) A214:482
4. Platt JR (1961) In: Flugge S (ed) Encyclopedia of physics. Springer, Berlin Göttingen Heidelberg, pp 171-240
5. Yen TF (1971) Theor Chim Acta 20:399
6. Herndon WC (1973) Tetrahedron 29:3; (1974) J Chem Ed 51:10
7. Randic M (1976) J Chem Soc Faraday Trans 2 72:232
8. Randic M (1980) Int J Quantum Chem 27:549
9. Cyvin SJ (1982) Monatsh Chemie 113:1127; (1983) 114:13
10. Trinajstic N (1983) Chemical graph theory II, chap. 2. CRC Press, Boca Raton, Florida
11. Fowler RH, Rushbrooke GS (1937) Trans Faraday Soc 33:1272
12. Read RC (1980) Fibonacci Quart 18:24
13. Hook JL, McQuistan RB (1983) J Math Phys 24:1859; (1984) Disc Appl Math 8:101
14. Phares AJ (1984) J Math Phys 25:1756
15. Nagle JF (1973) J Chem Phys 58:252; (1974) Proc Roy Soc (London) A337:569; (1975) Phys Rev Lett 34:1150; (1985) Phys Rev 31A:3199
16. Fisher ME (1984) J Stat Phys 34:667
17. Sachs H (1984) Combinations 4:89
18. Gutman I, Trinajstic N (1973) Croat Chem Acta 45:539
19. Cvetkovic D, Gutman I, Trinajstic N (1972) Chem Phys Lett 16:614;(1974) J Chem Phys 61:2700
20. Stein SE, Brown RL (1985) Carbon
21. Fisher ME (1961) Phys Rev 124:1664
22. Kasteleyn PW (1963) J Math Phys 4:287
23. Percus JK (1969) J Math Phys 10:1881
24. Lieb EH (1967) J Math Phys 8:2339
25. Hosoya H, Yamaguchi T (1975) Tetrahedron Lett 1975:4659
26. Gutman I, Randic M (1979) Chem Phys 41:265
27. Aihara J (1977) Bull Chem Soc Jpn 50:2010
28. Gutman I (1977) Theor Chim Acta 45:309; (1978) Bull Chem Soc Jpn 51:2729; (1981) Math Chem 11:127
29. Ohkami N, Motoyama A, Yamaguchi T, Hosoya H, Gutman I (1981) Tetrahedron 37:1113
30. Ohkami N, Hosoya H (1983) Theor Chim Acta 64:153
31. Wu FY (1968) Phys Rev 168:539
32. Baxter RJ (1970) J Math Phys 11:784
33. Gutman I, Randic M (1979) Chem Phys 41:265
34. Elser V (1984) J Phys A17:1509
35. There is a (one-to-two) correspondence between Kekulé structures on the honeycomb lattice and

the ground state to the antiferromagnetic Ising model on a triangular lattice. Thence the honeycomb-lattice Kekulé-structure count is given in terms of the zero-temperature entropy of this Ising model, a solution of which is given in Wannier GH (1950) Phys Rev 79:357
36. Harris FE, Randic M, Stolow R (unpublished work)
37. Dzonova-Jerman-Blazic B, Trinajstic N (1982) Comput and Chem 6:121
38. El-Basil S, Jashari G, Knop JV, Trinajstic N (1985) Monatsh Chemie 115:1299
39. Ramaraj R, Balasubramanian K (1985) J Comput Chem 6:122
40. Elser's (Ref. [34]) cases of enumeration were also given by Yen (Ref. [5]) and Elser's maximum per-site entropy case was given by Gordon and Davison (Ref. [2]); the methods of solution were quite different though
41. Klein DJ (1979) Int J Quantum Chem 13S:294
42. Seitz WA, Klein DJ, Schmalz TG, Garcia-Bach MA (1985) Chem Phys Lett 115:139
43. Klein DJ, Schmalz TG, Hite GE, Metropoulos A, Seitz WA (1985) Chem Phys Lett 120:367
44. Klein DJ, Schmalz TG, Seitz WA, Hite GE (1985) Int J Quantum Chem 19S
45. See, e.g., Gantmacher FR (1959) The theory of matrices, vol II, chap 13. Chelsea, New York
46. Pauling L (1960) The nature of the chemical bond, 3rd edn Cornell University Press, Ithaca, NY, pp. 236 ff; (1980) Acta Crystallogr B36:1898
47. Cruickshank DWJ, Sparks RA (1960) Proc Roy Soc (Lond) A258:270
48. Coulson CA (1970). In: Eyring H (ed) Physical chemistry: an advanced treatise 5. Academic Press, New York, pp 381 ff
49. Herndon WC (1974) J Am Chem Soc 96:7605